1 **Supplemental Information**

2 **Extended Results and Discussion**

3   To determine whether results from our animal studies showed translational

4 relevance to the human setting, we analyzed whether ILC percentages, with specific

5 interest in ILC2s, correlated in any way to carriage of known *NOD2* variants associated

6 with susceptibility to CD. We focused on the three main coding mutations in *NOD2*,

7 namely rs2066844 (single nucleotide polymorphism (SNP)8), rs2066845 (SNP12) and

8 rs2066847 (SNP13)(1), and evaluated ILC frequency in peripheral blood of 41 patients

9 with CD, 21 of whom were genotyped carriers of one or multiple *NOD2* SNPs (**Table**

10 **S5**). Our results show that frequencies of total ILCs were not significantly different

11 between carriers and non-carriers of all *NOD2* SNPs evaluated (**Fig. S2A**).

12 Furthermore, no significant differences were observed in the percentages of any of the

13 ILC subsets comparing CD-associated *NOD2* variant carriers with non-carriers (**Fig.**

14 **S2B**); specifically, in our CD patient population, carriage of either one or more of the

15 *NOD2* SNPs assayed (SNP8, SNP12, SNP13) did not alter the percentages any of the

16 ILC subsets compared to those measured in non-carriers (**Fig. S2C**). Relevant to the

17 present study, no direct effect of the *NOD2* SNPs was evident on the frequency of

18 ILC2s (**Fig. S2D**). Taken together, these preliminary findings did not show any

19 correlation(s) between carriage of CD-associated *NOD2/CARD15/IBD1* variants and

20 total ILC frequency, as well as specific ILC subsets, including ILC2s, in our CD patient

21 population evaluated.

22   These data, however, do not definitively rule out association between

23 *NOD2/CARD15/IBD1* variants and the presence of ILC2s, specifically during the

24   development of early disease, as indicated in our animal studies. As such, it is possible

25   that the impact of NOD2-sensing is critical at disease onset, and perhaps better

26   exemplified in newly diagnosed, treatment native CD patients. In addition, interrogation

27   of a larger patient sample size, and perhaps studies comparing ILCs derived from the

28   gut vs. systemic, circulating ILCs, as performed herein, are warranted and may reveal

29   different results than obtained in the present study. Importantly, we show for the first

30   time, using an established murine model of CD-like ileitis (*i.e.*, SAMP) that NOD2 has

31   the ability to regulate ILC2 expansion and function during the early stages of chronic

32   intestinal inflammation. Of note, using *Nod2*-deficient mice, Zhou *et al.* recently reported

33   that selective activation of ILC3s is also dependent on NOD2-sensing of the gut

34   microbiome by mucosal macrophages, which in turn, secrete IL-1β and induce ILC3s to

35   produce IL-2 that promotes Treg function and ultimate protection from chronic

36   inflammation(2). In the same study, reduced frequencies of both Tregs and IL-2-

37   producing ILC3s were detected in mucosal biopsies from CD patients vs. healthy

38   controls(2), although carriage of CD-associated *NOD2* variants and their potential

39   impact on ILC3 frequency and/or function (*i.e.*, IL-2 production) were not assessed in

40   their patient samples. As such, it is possible that NOD2 has simultaneous, yet opposing,

41   effects on different ILC subsets (*i.e.*, pathogenic vs. protective) in the pathogenesis of

42   CD. Taken together, emerging evidence supports the role of NOD2-dependent effects

43   on ILC expansion and function that are important in both gut health and disease. Future

44   studies are needed to uncover how these mechanism(s) can be harnessed to design

45   effective strategies to treat chronic intestinal inflammation, such as that observed in

46   IBD.

47 **Extended Methods**

48 *In vivo* **mouse studies.** All animal experiments were conducted in a blinded manner

49 without prior knowledge of experimental groups by experimenter (KGB/CDS), with mice

50 randomized to different interventions using progressive numeric labels, the code only

51 known to the animal caretaker (HLH), and revealed at end of studies. Scientific rigor,

52 data reproducibility and biological variables were followed based on recently published

53 guidelines(3). Blockade of IL-33 was achieved using 4-wk-old SAMP treated for 6-wks

54 with a murinized rat IgG1 Ab against mST2, with controls receiving an isotype IgG1 Ab

55 (both from Amgen, Seattle, WA); for IL-33 administration experiments, 10-wk-old AKR

56 and SAMP x $Nod2^{-/-}$ mice were injected with either murine rIL-33 (ALX-522-101; Enzo

57 Life Sciences, Farmingdale, NY) or PBS (vehicle control), as previously described(4).

58 For NOD2 activation studies, 10-wk-old GF-SAMP were treated i.p. for 3d with either

59 muramyl dipeptide (L18-MDP, 100ug/mouse) or endotoxin-free water (vehicle control),

60 both from InvivoGen, San Diego, CA, as previously reported(5).

61 **Tissue harvest, stereomicroscopy (SM)-assisted microdissection, and histologic**

62 **assessment.** Mice were euthanized and ileal tissues harvested and processed for

63 either histology, SM, qPCR, or lymphocyte isolation, as previously described(4,6,7).

64 MLNs were collected and single-cell suspensions prepared for either flow cytometry or

65 *ex vivo* functional assays(4,6,8). Ileal inflammation was histologically evaluated by a GI

66 pathologist in a blinded-fashion using an established scoring system(4,6). 3D-SM

67 Assessment and Pattern Profiling (3D-SMAPgut) was used to map and quantify extent

68 of mucosal disease in SAMPx$Nod2^{-/-}$ vs. WT ilea, with SM-assisted punch biopsy-

69 microdissection of involved and non-involved areas performed as previously

70   reported(7), with resulting tissues harvested for detection of IL-33 by qPCR and

71   Western blotting.

72   **Patient samples.** Intestinal (colonic/ileal) mucosal biopsies were collected from adult

73   patients with confirmed diagnosis of CD and from healthy controls, included upon

74   negative endoscopic findings during polyp screen. Additional biopsies were taken from

75   resected specimens of patients undergoing hemicolectomy for either stricturing CD to

76   obtain inflamed/non-inflamed ileal tissues or colorectal cancer to obtain non-inflamed

77   healthy control tissues from margins (**Table S2**, **S3** and **S5**). Specifically, six mucosal

78   biopsies were taken from macroscopically involved lesions in CD patients. In healthy

79   individuals, colonic biopsies were taken randomly, mainly from the splenic flexure.

80   Biopsies were collected in sterile RPMI 1640 medium (Lonza Bioscience, Basel,

81   Switzerland) and stored at 4°C until processing (within 1h).

82   Combined biopsies were subsequently washed in RPMI supplemented with

83   HEPES (Lonza Bioscience), 10% FBS and 2% antibiotic-antimycotic (both

84   ThermoFisher, Waltham, MA). Epithelium was removed by incubation in RPMI-

85   supplemented with EDTA (Lonza Bioscience), DTT (Chem Lab, Zedelgem, Belgium)

86   and HEPES at 37 °C on a magnetic stirrer at 400 rpm for 20min. Resulting tissues were

87   transferred to 5 mL HBSS with calcium and magnesium (Lonza Bioscience)

88   supplemented with HEPES, FBS, 5.0mg collagenase IV (Worthington Biochemical

89   Corp., Lakewood, NJ) and 10 µl DNase I (Roche, Penzburg, Germany) at 37 °C on a

90   magnetic stirrer at 400 rpm for 40min. Cell suspensions were strained through 70µm

91   filters (EASYstrainer™, Greiner Bio-One, Monroe, NC), quenched with 5 ml PBS with

92   2.5% BSA, and centrifuged at 400g for 5min. Remaining undigested tissues were again

93 resuspended in 5 mL HBSS supplemented with HEPES, FBS, 5.0 mg collagenase and

94 10µl DNase I at 37 °C on a magnetic stirrer at 400 rpm for 20 min.

95 **Flow cytometry.** Single-cell suspensions of MLN- and ileal lamina propria-derived

96 lymphocytes were isolated from experimental mice and either assayed immediately or

97 prepared for *ex vivo* stimulation experiments, as described before[4,6,8] and using the

98 Lamina Propria Dissociation Kit (Miltenyi Biotec, Waltham, MA) according to

99 manufacturer's instructions, respectively. For cell-surface staining, $2x10^6$ cells were

100 incubated with fixable live/dead cell dye in violet or aqua (ThermoFisher), Fc-receptors

101 blocked with anti-CD16/CD32 (eBioscience, San Diego, CA), and stained for 30min at

102 4°C with indicated antibodies (**Table S4**). For intracellular staining, cells were fixed in

103 Fix/Perm and Permeabilization Buffers (eBioscience) for 30min each at 4°C and RT,

104 respectively, in presence of indicated antibodies (**Table S4**). Absolute numbers of gut

105 mucosal cells were calculated using CountBright^{TM} Absolute Counting Beads

106 (Invitrogen, Carlsbad, CA). For compensation, flow minus one controls and single

107 stained beads from AbC Total Antibody Compensation Bead Kit (Invitrogen) were used.

108 Total ILCs and ILC subsets in experimental mice were identified using standard gating

109 strategies (**Figure 1A,D**).

110   For ILC2 functional assays, single cell suspensions were isolated as described

111 above and incubated *ex vivo* ($2x10^6$ cells/well) in the presence of BD GolgiPlug Protein

112 Transport Inhibitor (containing Brefeldin A) with/without Leukocyte Activation Cocktail

113 (containing PMA/ionomycin) for 5h at 37°C in 5%CO_2, according to manufacturer's

114 instructions (Becton Dickinson, San Jose, CA). Cells were then stained for cell-surface

115 markers and intracellular IL-5, as described above. Cells/data were acquired on FACS

116 Aria or LSR II instruments, and analyzed with FlowJo Software (all Becton Dickinson).

117   For human studies, viability of isolated leukocytes derived from gut mucosal

118 biopsies (**Tables S2, S3 and S5**) was determined with Fixable Viability Dye (FVD780,

119 Biolegend, San Diego, CA), and intestinal leukocytes (4×10^6) were stained with

120 indicated Abs (**Table S4**) in 100 µl PBS/BSA supplemented with human serum and

121 Brilliant Stain Buffer (563794, Becton Dickinson), and fixed for 10min in 0.5% PFA.

122 Cells were resuspended in PBS/BSA/EDTA and stored at 4°C in dark until acquisition

123 on an LSR Fortessa instrument, with calibration performed by CS&T beads (all from

124 Becton Dickinson). For compensation controls, single color UltraComp eBeads™

125 (ThermoFisher) were used, and Fluorescence Minus One (FMO) controls included.

126 Total ILCs are defined as $Lin^-CD161^+CD127^+$ cells within live $CD45^+$ population. Among

127 total ILCs, ILC2s were further identified as $CRTH2^+$ ($CD294^+$), NCR^-ILC3s as $CRTH2^-$

128 $CD117^+NKp44^-/CD336^-$, NCR^+ILC3s as $CRTH2^-$ $CD117^+NKp44^+$, and ILC1s as $CRTH2^-$

129 $CD117^-NKp44^-$ (**Figure 4A**).

130 **Genotyping for *NOD2* variants.** DNA was extracted from peripheral blood leukocytes

131 and genotyping performed as previously described(9). Briefly, CD patients and healthy

132 controls (**Table S5**) were evaluated for carriage of the three main CD-associated *NOD2*

133 variants p.Arg702Trp (rs2066844), p.Gly908Arg (rs2066845) and p.Gly908Arg

134 (rs2066847)(1); haplotype and genotype-phenotype (ILC frequency) analyses were

135 subsequently performed.

136   **Statistics.** Data included in Supplemental Information were analyzed using GraphPad

137   Prism 5 (GraphPad Software, La Jolla, CA). Selection of appropriate statistical tests

138   was based on variance and underlying distribution of data. Global effects between

139   groups were first assessed using one-way ANOVA with Bonferroni correction for

140   multiple comparisons. Differences between individual groups were directly compared as

141   indicated in each supplemental figure legend, with $P \leq 0.05$ considered significant.

142   **References**

143   1. Hampe J, et al. Association of NOD2 (CARD 15) genotype with clinical course of

144   Crohn's disease: a cohort study. *Lancet.* 2002;359(9318):1661-5.

145   2. Zhou L, et al. Innate lymphoid cells support regulatory T cells in the intestine through

146   interleukin-2. *Nature.* 2019;568(7752):405-9.

147   3. Arseneau KO, Cominelli F. Improving the reproducibility and quality of reporting for

148   animal studies in inflammatory bowel disease. *Inflamm Bowel Dis.*

149   2017;23(12):2069-71.

150   4. De Salvo C, et al. IL-33 drives eosinophil infiltration and pathogenic type 2 helper T-

151   cell immune responses leading chronic experimental ileitis. *Am J Pathol.*

152   2016;186(4):885-98.

153   5. Corridoni D, et al. Dysregulated NOD2 predisposes SAMP1/YitFc mice to chronic

154   intestinal inflammation. *Proc Natl Acad Sci USA.* 2013;110(42):16999-7004.

155   6. Pastorelli L, et al. Epithelial-derived IL-33 and its receptor ST2 are dysregulated in

156   ulcerative colitis and in experimental Th1/Th2 driven enteritis. *Proc Natl Acad Sci*

157   *USA.* 2010;107(17):8017-22.

158   7. Rodriguez-Palacios A, et al. Stereomicroscopic 3D-pattern profiling of murine and

159   human intestinal inflammation reveals unique structural phenotypes. *Nat Commun.*

160   2015;6:7577.

161   8. Sonnenberg GF, Monticelli LA, Elloso MM, Fouser LA, Artis D. CD4(+) lymphoid

162   tissue-inducer cells promote innate immunity in the gut. *Immunity.* 2011;34(1):122-

163   34.

164 9. Vancamelbeke M, et al. Genetic and transcriptomic bases of intestinal epithelial

165   barrier dysfunction in inflammatory bowel disease. *Inflamm Bowel Dis.*

166   2017;23(10):1718-29.

167 10. Takayama T, et al. Imbalance of NKp44(+)NKp46(-) and NKp44(-)NKp46(+) natural

168   killer cells in the intestinal mucosa of patients with Crohn's disease. *Gastroenterol.*

169   2010;139(3):882-92.

170 11. Geremia A, et al. IL-23-responsive innate lymphoid cells are increased in

171   inflammatory bowel disease. *J Exp Med.* 2011;208(6):1127-33.

172 12. Bernink JH, et al. Human type 1 innate lymphoid cells accumulate in inflamed

173   mucosal tissues. *Nat Immunol.* 2013;14(3):221-9.

174 13. Fuchs A, et al. Intraepithelial type 1 innate lymphoid cells are a unique subset of IL-

175   12- and IL-15-responsive IFN-γ-producing cells. *Immunity.* 2013;38(4):769-81.

176 14. Longman RS, et al. CX_3CR1^+ mononuclear phagocytes support colitis-associated

177   innate lymphoid cell production of IL-22. *J Exp Med.* 2014;211(8):1571-83.

178 15. Mizuno S, et al. Cross-talk between RORγt[+] innate lymphoid cells and intestinal

179   macrophages induces mucosal IL-22 production in Crohn's disease. *Inflamm Bowel*

180   *Dis.* 2014;20(8):1425-34.

181 16. Bernink JH, et al. Interleukin-12 and -23 control plasticity of CD127(+) group 1 and

182   group 3 innate lymphoid cells in the intestinal lamina propria. *Immunity*.

183   2015;43(1):146-60.

184 17. Hepworth MR, et al. Immune tolerance. Group 3 innate lymphoid cells mediate

185   intestinal selection of commensal bacteria-specific CD4^{+} T cells. *Science.*

186   2015;348(6238):1031-5.

187   18. Lim AI, et al. IL-12 drives functional plasticity of human group 2 innate lymphoid

188   cells. *J Exp Med.* 2016;213(4):569-83.

189   19. Li J, Doty AL, Iqbal A, Glover SC. The differential frequency of Lineage(-)CRTH2(-

190   )CD45(+)NKp44(-)CD117(-)CD127(+) ILC subset in the inflamed terminal ileum of

191   patients with Crohn's disease. *Cell Immunol.* 2016;304-305:63-8.

192   20. Li J, et al. Enrichment of IL-17A$^+$IFN-γ^+ and IL-22$^+$ T cell subsets is associated with

193   reduction of NKp44$^+$ ILC3s in the terminal ileum of Crohn's disease patients. *Clin*

194   *Exp Immunol.* 190(1):143-53.

195   21. Forkel M, et al. Distinct alterations in the composition of mucosal innate lymphoid

196   cells in newly diagnosed and established Crohn's disease and ulcerative colitis. *J*

197   *Crohns Colitis.* 2019;13(1):67-78.

198   **Supplemental Figure Legends**

199   **Figure S1.** ***Group 2 ILCs remain the predominant ILC subset as ileitis progresses***

200   ***into established disease in SAMP mice.*** **A)** Representative H&E-stained histologic

201   images of ilea from 4-, 10- and 20-wk-old AKR (parental control) mice depict

202   development of healthy ileal tissues with formation of normal crypt-villous structures and

203   minimal baseline levels of inflammatory cells (*upper row*). In contrast, while 4-wk-old

204   SAMP (similar to age-matched AKR) show no histologic evidence of inflammation

205   (*lower left*), infiltration of inflammatory cells within the lamina propria with expansion and

206   flattening of villi, and hypertrophy of muscular layers begins to manifest at 10-wks (*lower*

207   *middle*). At 20-wks, frank villous blunting with dramatic changes in crypt-villous

208   architecture becomes apparent, with marked presence of goblet cells and severe

209   inflammation (crypt abscess with encased neutrophils noted in center of field, *lower*

210   *right*), characteristic of SAMP (scale bar=100μm). **B)** Time course of ileal disease

211   severity in SAMP vs. AKR (*n*=10-13). **C)** Although total ILC frequency within live CD45$^+$

212   population remains stable as ileitis is established and adaptive immune cells expand at

213   20-wks in SAMP (**Fig. 1A**), increased ILC2 percentages persist (*left*) and absolute

214   numbers significantly rise (*right*) compared to age-matched AKR (*n*=5). **D)**

215   Representative H&E-stained histologic images of ilea from WT SAMP (SAMPx*Rag2*$^{+/+}$,

216   *upper row*) compared to SAMP lacking T/B-lymphocytes, but with intact innate immune

217   function (SAMPx*Rag2*$^{-/-}$, *lower row*), at 4-, 10- and 20-wks of age. While SAMPx*Rag2*$^{+/+}$

218   develop ileitis over a similar time course to native SAMP (**A,B**), SAMPx*Rag2*$^{-/-}$ show

219   marked, active inflammation at 10-wks, with similar severity to WT SAMP (**Figure 1F**),

220   which persists at 20-wks, but is dramatically reduced compared to WT and native SAMP

221 (scale bar=100μm). **$P \le 0.01$, ***$P \le 0.001$, ****$P \le 0.001$, and ($^{####}P \le 0.001$ vs. 4-wk-old

222 SAMP) by two-tailed unpaired Student's *t*-test; experiments performed at least in

223 duplicate.

224 **Figure S2.** *__Association of NOD2 variants and ILC frequencies in Crohn's disease__.*

225 **A)** Frequency of total ILCs (Lin⁻CD161⁺CD127⁺) within live CD45⁺ population in CD

226 patients who are carriers of one or more allele variants for either SNP8, SNP12 or

227 SNP13 compared to non-carriers. **B)** Percentages of (●)ILC1s (CD294⁻CD117⁻CD336⁻),

228 (●)ILC2s (CD294⁺), and (●)ILC3s (CD294⁻CD117⁺CD336⁻) of total ILCs comparing

229 carriers (≥1 SNP) vs. non-carriers, and **C)** broken down by number of affected regions

230 (SNP8-12-13). **D)** Frequency of ILC2s comparing carriers vs. non-carriers of *NOD2*

231 variant rs2066844 (SNP8), rs2066845 (SNP12), and rs2066847 (SNP13) in CD

232 patients. Data presented as box plots (25th, 50th, 75th quantiles shown); *N*=41. No

233 significant differences were observed between carriers (≥1) and non-carriers (0) of

234 *NOD2* variants by unpaired nonparametric Mann-Whitney test, and among carriers of 0-

235 1-2-3 SNPs by one-way ANOVA with Bonferroni correction.

236 **Table S1.** *Human studies supporting contribution of ILCs to the pathogenesis of IBD.*

Patients	Study design	ILC1	ILC2	ILC3	Summary	Ref.
IBD	Surgically-resected colons from moderate-to-severe CD, UC and unaffected areas of colon cancer (control)	-	-	↑	Imbalance of NKp44^{+}/NKp46^{+} cells in CD, with ↑IFNγ-producing NKp46^{+} cells vs. control	10
IBD	Blood from CD, UC, surgically-resected ilea/colons and mucosal biopsies from CD and healthy areas of CRC (control)	↑	-	**-**	↑IL-17^{+}IFNγ^{+} IL-23-responding CD56^{-} ILCs in gut, but not peripheral blood, of CD vs. UC and control	11
CD	Surgically-resected inflamed ilea from CD and from unaffected ilea from colon cancer (non-inflamed control)	↑	-	↓	↑IFNγ-expressing ILC1s and ↓NKp44^{+} ILC3s in active CD vs. control	12
CD	Surgically-resected non-inflamed colons and small intestines from CD and non-IBD patients (control)	↑	-	-	↑intraepithelial IFNγ/CCL4-producing NKp44^{+}CD103^{+} ILC1s in CD vs. non-IBD control	13
IBD	Biopsies from descending colon of mild-to-moderate CD, UC and non-IBD undergoing routine screening (control)	-	-	↑	↑protective IL-22-producing ILC3s in CD and UC vs. control, regulated by IL-23/IL-1β/TL1A-producing CX_3CR1^+ MNPs	14
CD	Surgically-resected affected and unaffected (control) intestines from moderate-to-severe CD	-	-	NC	No change in percentages RORγt^{+}CD127^{+}CD56^{-}/CD56^{+} ILC3s in inflamed vs. non-inflamed CD, but ↑IL-22 from these cells in non-inflamed CD when co-cultured with inflammatory macrophages	15
CD	Surgically-resected inflamed ilea from CD and unaffected ilea from colon cancer (non-inflamed control)	↑	-	↓	↑IFNγ-producing CD127^{+} ILC1s at cost of IL-22-producing NKp44^{+} ILC3s in CD vs. control, which is reversible in presence of IL-2, IL-23, and IL-1β that is dependent on RORγt and enhanced by RA; plasticity also dependent on CD14^{+/-} DCs	16
CD	Intestinal biopsies from right and left colons of pediatric CD and non-IBD patients (control)	-	-	NC	↓MHCII on colonic ILC3s (but no change in ILC3 frequency) in CD vs. non-IBD associates with elevated commensal bacteria-specific inflammatory responses	17
CD	Ileocecal resections from refractory CD compared to peripheral blood from healthy donors (control)	-	↑	-	↑IL-13^{+} ILC2s that co-express IFNγ in CD gut vs. peripheral blood (not gut-derived, however) from normal donors, suggesting plasticity of ILC2s in context of IBD	18
CD	Surgically-resected terminal ilea from CD patients (various degree of inflammation)	↑	-	↓	↑Lin^{-}CRTH2^{-}CD45^{+}NKp44^{-}CD117^{-}CD127^{+} and ↓Lin^{-}CRTH2^{-}CD45^{+}NKp44[+/-]CD117^{+}CD127^{+} ILCs with	19

					increased CD severity that is reversible after ustekinumab (anti-IL-12/IL-23) treatment	
CD	Surgically-resected inflamed and unaffected areas from terminal ilea of CD patients who failed medical treatment	↑	-	↓	↑NKp44⁻CD117⁻ ILC1s and ↓(HLA-DR) NKp44⁺ ILC3s associated with ↑pathogenic IL-17A⁺IFNγ⁺ and IL-22⁺IFNγ⁺ T cell subsets	20
IBD	Blood and inflamed/non-inflamed ileal/colonic biopsies from newly diagnosed and ≥1y CD, UC and patients undergoing tumor screening found to be negative (non-IBD control)	↑	↑	↓	↓NKp44⁺ ILC3s and ↑ILC1s, ILC2s and NKp44⁻ ILC3s correlates with ↑IBD severity. ↑ILC1s and ↑ILC2s in newly diagnosed CD and UC, respectively, with both ↑ILC1s and ILC2s in established IBD. No change in circulating ILC frequency after vedolizumab (anti-α4β7) treatment	21
CD	Surgically-resected inflamed/non-inflamed small intestines from CD and ileal biopsies from pediatric CD and non-IBD controls	-	-	↓	IL-1β-ILC3-IL-2 circuit essential for Treg maintenance and small intestinal homeostasis. ↓IL-2⁺ ILC3s correlates with ↓Treg frequency in CD	2
IBD	Blood at baseline and at weeks 0, 4, 8, 14/24 after biological therapy; colonic biopsies at baseline from edge of inflamed ulcers and from sigmoid of healthy controls	↓		↑	Intestinal, but not circulating, ILCs are impacted by biological therapy. ↑NKp44⁺ ILC3s and ↓ILC1 after biological therapy as collateral effect of intestinal healing	22
IBD	Blood and/or colonic tissues from pediatric and adult subjects with active disease	↓↑		↓	↓ILC1s in blood of CD, but ↑ in mucosa of CD>UC. ↓ILC3s in UC mucosa	23

237 **Abbreviations: CD**, Crohn's disease; **CRC**, colorectal cancer; **CRTH2**, chemoattractant receptor-homologous molecule expressed on Th2 cells; **IBD**,
238 inflammatory bowel disease; **ILC**, innate lymphoid cells; **ILC1-3**, group 1-3 innate lymphoid cells; **Lin⁻**, lineage negative; **MNPs**, mononuclear phagocytes; **NC**, no
239 change; **RA**, retinoic acid; **RORγt**, retinoic acid receptor-related orphan receptor-γt; **TL1A**, TNF-like factor 1A; **UC**, ulcerative colitis

240 **Table S2.** *Demographics of CD patients (active) and healthy controls.*

	CD	HC
Number of patients (*N*)	56	24
Sex, women, *n* (%)	29 (51.8%)	14 (58.3%)
Age (yrs), mean (±SEM)	40.0 (±2.3)	57.8 (±2.8)
Disease duration (yrs), mean (±SEM)	14.06 (±1.5)	-
Disease location, *n* (%)		
Ileal (L1)	17 (30.4%)	6 (25%)
Colonic (L2)	11 (19.6%)	18 (75%)
Ileocolonic (L3)	27 (48.2%)	-
NA	1 (0.02%)	-

241 **Abbreviations: CD**, Crohn's disease; **HC**, healthy controls; **NA**, no answer

242   **Table S3.** *Demographics of ileal-specific CD patients (matched samples).*

	CD
Number of patients (*N*)	10
Sex, women, *n* (%)	5 (50.0%)
Age (yrs), mean (±SEM)	53.6 (±3.9)
Disease duration (yrs), mean (±SEM)	20.4 (±4.6)
Medications (at time of tissue procurement), *n* (%)	
Steroids	1 (10.0%)
Anti-TNF (Adalimumab, IFX)	2 (20.0%)
Ustekinumab	2(20.0%)
Vedolizumab	1 (10.0%)
MTX	1(10.0%)
None	3 (30.0%)

243   **Abbreviations: CD**, Crohn's disease; **IFX**, Infliximab; **MTX**, methotrexate

244   **Table S4.** *Antibodies utilized for flow cytometry.*

Antibody (raised against)		Label	Clone/ Catalog #	Source
Antigen	**Species**			
CD45	mouse	PerCP	30-F11	eBioscience, San Diego CA
CD127	mouse	eFluor480	A7R34	eBioscience
ST2/IL-33R	mouse	FITC	DJ8	mdBiosciences, Zurich Switzerland
Lineage markers[A]	mouse	FITC	# 133301	Biolegend, San Diego, CA
Lineage markers[B]	mouse	eFluor450	# 133313	Biolegend
T-bet	mouse	PE-Cy7	4B10	eBioscience
GATA3	mouse	PE	TWAJ	eBioscience
RORγt	mouse	APC	AFKJS-9	eBioscience
IL-5	mouse	BV 421	TRFK5	Biolegend
CD11c	human	FITC	3.9	ThermoFisher, Waltham, MA
CD123	human	FITC	6H6	ThermoFisher
CD14	human	FITC	61D3	ThermoFisher
CD19	human	FITC	HIB19	ThermoFisher
CD1a	human	FITC	HI149	ThermoFisher
CD3	human	FITC	UCHT1	ThermoFisher
CD303a	human	FITC	201A	ThermoFisher
CD94	human	FITC	DX22	ThermoFisher
FceRIa	human	FITC	AER-37 (CRA1)	ThermoFisher
TCRα/β	human	FITC	IP26	ThermoFisher
TCRγ/δ	human	FITC	B1.1	ThermoFisher
CD34	human	FITC	4H11	ThermoFisher
CD45	human	AF 700	2D1	ThermoFisher
CD161	human	PE-Cy7	HP-3G10	ThermoFisher
CD117	human	BV 421	YB5.B8 (RUO)	BD Biosciences, San Jose, CA
CD127	human	BV 711	A019D5	Biolegend
CD294	human	AF 647	BM16	Biolegend
CD336	human	PE	P44-8	Biolegend
CD4	human	eVolve 605	SK3	ThermoFisher

245   **Abbreviations: AF**, Alexa Fluor; **APC**, allophycocyanin; **BV**, brilliant violet; **GATA3**, GATA binding
246   protein-3; **PerCP**, peridinin-chlorophyll-protein; **PE/PE-Cy7**, R-phycoerythrin (coupled to cyanin dye);
247   **RORγt**, retinoic acid receptor-related-orphan-receptor-gamma t; **T-bet**, T-box expressed in T cells)

248   [A]**CD3e** (145-2C11), **Ly-6G/Ly-6C** (RB6-8C5), **CD11b** (M1/70), **CD45R/B220** (RA3-6B2), **TER-**
249   **119/Erythroid cells** (Ter-119); [B]**CD3** (17A2), **Ly-6G/Ly-6C** (RB6-8C5), **CD11b** (M1/70), **CD45R/B220**
250   (RA3-6B2), **TER-119/Erythroid cells** (Ter-119

251

252 **Table S5.** *Demographics of CD patients (NOD2 variant non-carriers vs. carriers).*

	Non-carriers (0)	Carriers (≥1)
Number of patients (*N*)	20	21
Sex, women, *n* (%)	13 (65.0%)	13 (61.9%)
Age (yrs), mean (±SEM)	45.1 (±3.8)	46.42 (±2.5)
Disease location, *n* (%)		-
Ileal (L1)	9 (45.0%)	7(33.3%)
Colonic (L2)	1 (5.0%)	4(19.0%)
Ileocolonic (L3)	10 (50.0%)	10(47.6%)

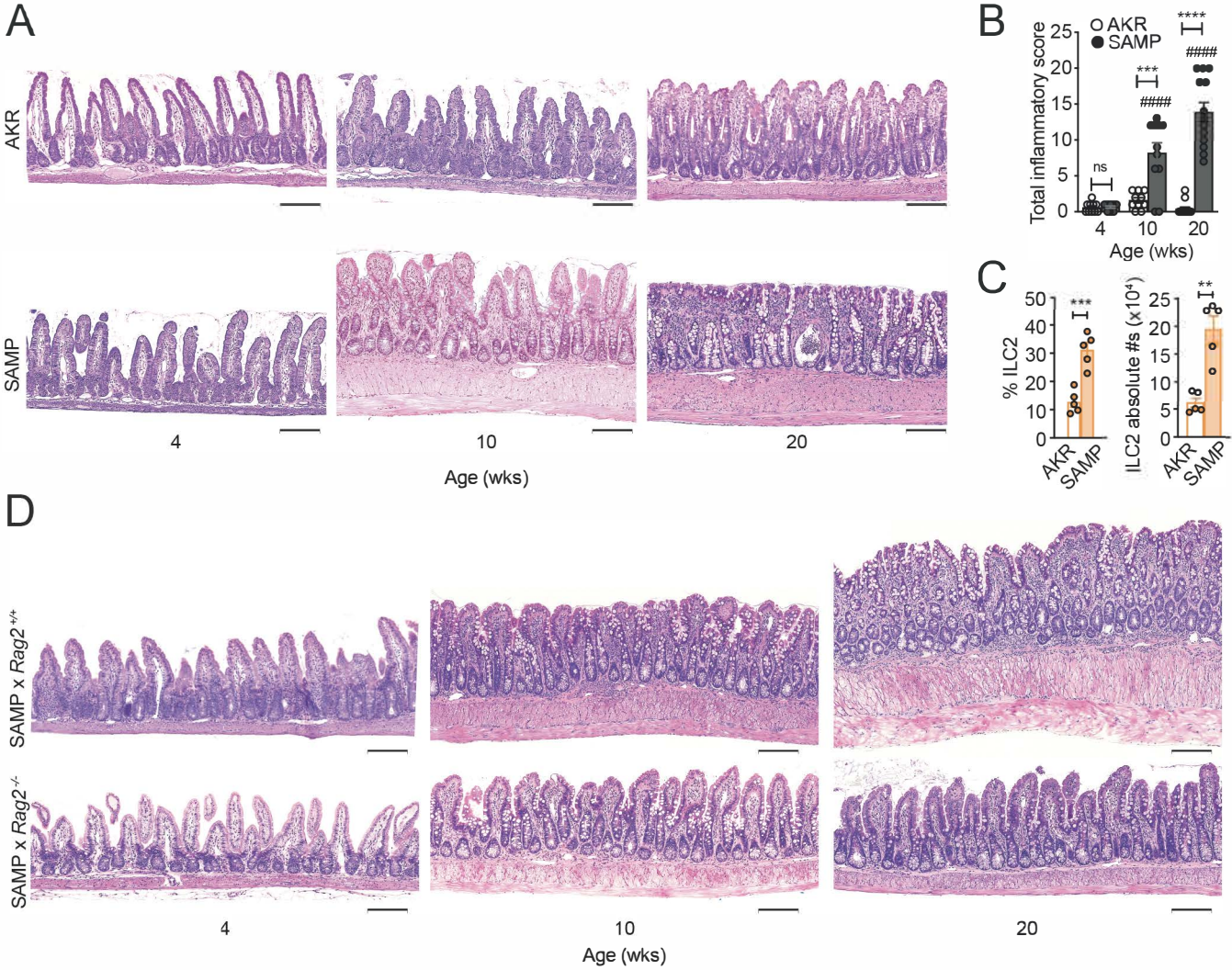253 **Abbreviations: CD**, Crohn's disease; **HC**, healthy controls

Figure S1. _Group 2 ILCs remain the predominant ILC subset as ileitis progresses into established disease in SAMP mice_. **A)** Representative H&E-stained histologic images of ilea from 4-, 10- and 20-wk-old AKR (parental control) mice depict development of healthy ileal tissues with formation of normal crypt-villous structures and minimal baseline levels of inflammatory cells (_upper row_). In contrast, while 4-wk-old SAMP (similar to age-matched AKR) show no histologic evidence of inflammation (_lower left_), infiltration of inflammatory cells within the lamina propria with expansion and flattening of villi, and hypertrophy of muscular layers begins to manifest at 10-wks (_lower middle_). At 20-wks, frank villous blunting with dramatic changes in crypt-villous architecture becomes apparent, with marked presence of goblet cells and severe inflammation (crypt abscess with encased neutrophils noted in center of field, _lower right_), characteristic of SAMP (scale bar=100μm). **B)** Time course of ileal disease severity in SAMP vs. AKR (_n_=10-13). **C)** Although total ILC frequency within live CD45$^+$ population remains stable as ileitis is established and adaptive immune cells expand at 20-wks in SAMP (**Fig. 1A**), increased ILC2 percentages persist (_left_) and absolute numbers significantly rise (_right_) compared to age-matched AKR (_n_=5). **D)** Representative H&E-stained histologic images of ilea from WT SAMP (SAMPx _Rag2$^{+/+}$_, _upper row_) compared to SAMP lacking T/B-lymphocytes, but with intact innate immune function (SAMPx_Rag2$^{-/-}$_, _lower row_), at 4-, 10- and 20-wks of age. While SAMPx_Rag2$^{+/+}$_ develop ileitis over a similar time course to native SAMP (**A,B**), SAMPx_Rag2$^{-/-}$_ show marked, active inflammation at 10-wks, with similar severity to WT SAMP (**Figure 1F**), which persists at 20-wks, but is dramatically reduced compared to WT and native SAMP (scale bar=100μm). **P≤0.01, ***P≤0.001, ****P≤0.001, and (####P≤0.001 vs. 4-wk-old SAMP) by two-tailed unpaired Student's _t_-test; experiments performed at least in duplicate.
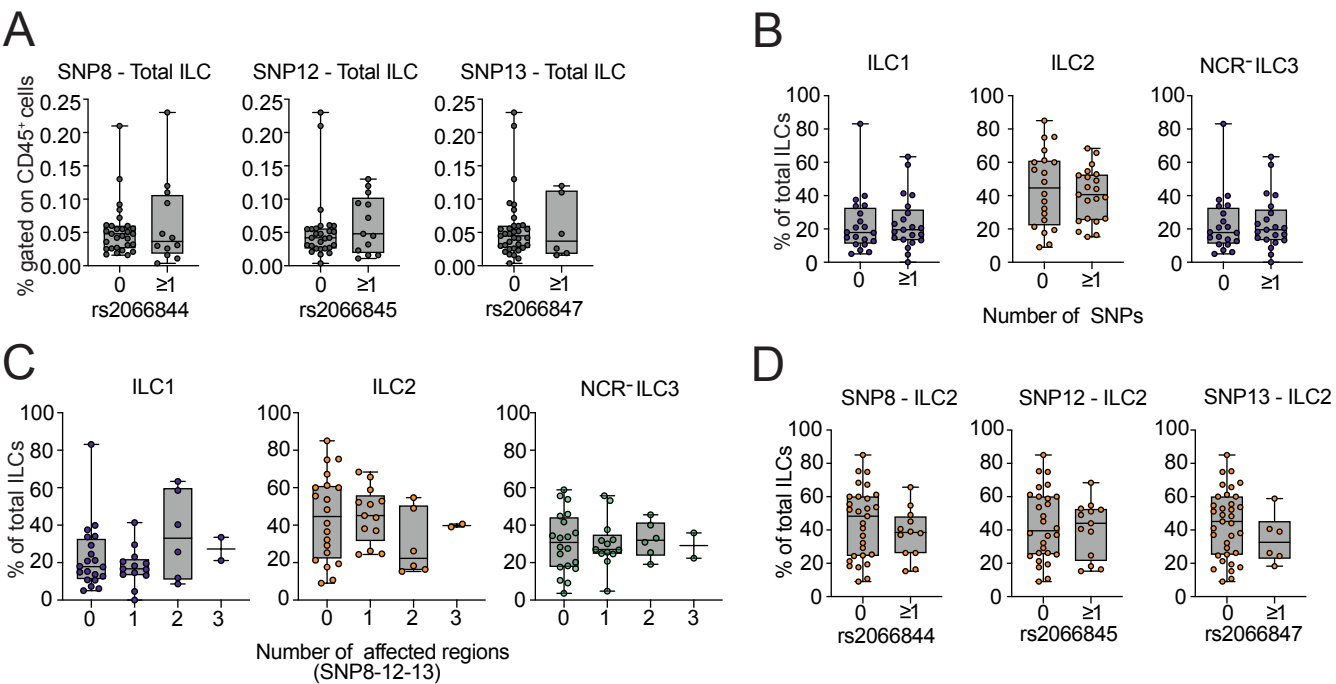
Figure S2. _Association of NOD2 variants and ILC frequencies in Crohn's disease_.
A) Frequency of total ILCs (Lin⁻CD161⁺CD127⁺) within live CD45⁺ population in CD patients who are carriers of one or more allele variants for either SNP8, SNP12 or SNP13 compared to non-carriers. **B)** Percentages of ILC1s (CD294⁻CD117⁻CD336⁻), ILC2s (CD294⁺), and ILC3s (CD294⁻CD117⁺CD336⁻) of total ILCs comparing carriers (≥1 SNP) vs. non-carriers, and **C)** broken down by number of affected regions (SNP8-12-13). **D)** Frequency of ILC2s comparing carriers vs. non-carriers of _NOD2_ variant rs2066844 (SNP8), rs2066845 (SNP12), and rs2066847 (SNP13) in CD patients. Data presented as box plots (25th, 50th, 75th quantiles shown); _N_=41. No significant differences were observed between carriers (≥1) and non-carriers (0) of _NOD2_ variants by unpaired nonparametric Mann-Whitney test, and among carriers of 0-1-2-3 SNPs by one-way ANOVA with Bonferroni correction.